PERGAMON

International Journal of Solids and Structures 39 (2002) 4167–4180

INTERNATIONAL JOURNAL OF SOLIDS and STRUCTURES

www.elsevier.com/locate/ijsolstr

Enhancing flutter and buckling capacity of column by piezoelectric layers

Q. Wang *, S.T. Quek

Department of Civil Engineering, National University of Singapore, Engineering Drive 2, Singapore 117576, Singapore

Received 26 November 2001; received in revised form 11 April 2002

Abstract

This paper illustrates the use of a pair of piezoelectric layers in increasing the flutter and buckling capacity of a column subjected to a follower force. The column is fixed at one end while the other one is free to rotate but constrained transversely by a spring. The mathematical formulation is presented and solved numerically. The effect of the spring stiffness on the capacity and type of instability of the column is first illustrated numerically for the case without any piezoelectric actuators. A transition value for the stiffness can be identified, below which the column fails by flutter and above which the column buckles. Next, an external voltage is applied on the piezoelectric layers bonded on the surfaces of the column, which induces locally a pair of tensile follower force. This has the effect of increasing the capacity of the column as the voltage increases while the transition stiffness remains virtually unchanged for a given size and location of piezoelectric actuators. It is also shown that the capacity of the column increases with longer layers for a fixed voltage. However, the location of the layers along the column determines the transition stiffness and hence has an effect on the type of failure for a fixed spring constant. Positioning towards the fixed end increases the flutter capacity whereas positioning away will result in an increase in buckling capacity.
© 2002 Elsevier Science Ltd. All rights reserved.

Keywords: Piezoelectric actuators; Column; Flutter; Buckling; Follower force

1. Introduction

Flutter and buckling are the two main forms of instability of column structures. The mathematical solution for the buckling analysis of columns under different boundary conditions subjected to non-follower compression is well documented in the monograph by Timoshenko and Gere (1961). A non-follower force is usually referred as an axial force with its direction remaining constant during the deformation of the structure. Buckling of a column is referred as the change of its equilibrium state from one configuration to another at a critical compressive load. On the other hand, flutter refers to the phenomenon where the amplitude of vibration of the column due to an initial disturbance grows without limit.

* Corresponding author. Tel.: +65-874-4683; fax: +65-779-1635.
E-mail address: cvewangq@nus.edu.sg (Q. Wang).

0020-7683/02/$ - see front matter © 2002 Elsevier Science Ltd. All rights reserved.
PII: S0020-7683(02)00334-7

A classical problem attracting considerable interests was the stability of a column fully fixed at one end and subjected to a tangential compressive (or follower) force at the other free end (Bolotin, 1963). A follower force is different from the non-follower force mentioned above in the sense that the direction of this type of force remains tangent to the deflection curve at the top of the column. Feodos'ev (1953) and Pfluger (1950) could not find any forms of equilibrium close to the undeformed position and concluded erroneously that a column under a follower force is always stable. It is Beck (1952) who first solved this instability problem based on dynamic analysis. The flutter of column under a follower force is usually referred as problem of Beck's column and this problem has been received considerable interests and development. Hauger and Vetter (1976) studied the influence of Winkler's elastic foundation on the stability of Beck's column. The influence of a pulsating force was investigated by Atanackvic and Cveticanin (1994) while the optimal shape of Beck's column was solved by Hanaoka and Washizu (1979). Matsuda et al. (1993) analyzed the effect of variable cross-section and shear stress on the value of the critical force. It is well-known that the buckling capacity of a propped cantilever is $p = \pi^2 EI/(0.699L)^2 \approx 2.045\pi^2 EI/L^2$ both for follower compression and non-follower compression force (Timoshenko and Gere, 1961; Beck, 1952). Kounadis (1983) studied the mathematical solution to the case of a column fixed at one end and constrained by a linear spring with stiffness k at the other end. It is shown that if k is low, the column will fail by flutter whereas above a transition value, buckling failure will occur.

The applications of the smart materials in engineering structures have drawn serious attention recently. Loughlan (1996) attempted to maintain the original shape of structures in order to avoid buckling and the subsequent adverse effect of post-buckling behaviour using shape memory alloys (SMA). Although SMA is capable of actuating a significant force, its slow response time hinders its usage in certain circumstances. On the other hand, the piezoelectric materials are light and able to provide rapid response through electromechanical coupling. Such materials have been studied in varied applications such as shape control of structures, acoustic wave excitation and structural health monitoring (Milsom et al., 1977; Monkhouse et al., 2000; Morgan, 1998). However, the research on using piezoelectric materials to enhance the stability of structures has not attracted much attention from the scientific community.

Chandrashekhara and Bhatia (1993) developed a finite element model for the active buckling control of laminated composite plates with surface bonded or embedded piezoelectric sensors that are either continuous or segmented. The dynamic buckling behaviour of the laminated plate subjected to a linearly increasing compression load is investigated in their work. Chase and Bhashyam (1999) derived optimal design equations to actively stabilize laminated plates loaded above the critical buckling load using a large number of sensors and actuators. Such work finds applications in aircraft wing skins. Meressi and Paden (1993) showed that the buckling of a flexible beam could be postponed beyond the first critical load by means of feedback using piezoelectric actuators and strain gauges. The problem of spill over was also discussed. Thompson and Loughlan (1995) studied experimentally the potential to increase the load bearing strength of imperfection sensitive composite columns loaded in compression. The concept is to apply a controlled voltage to the actuators to induce a reactive moment at the column centre with the aim of removing the lateral deflections and force the column to behave in a perfectly straight manner. The use of piezoelectric layers to induce tensile forces on the host column in enhancing the buckling capacity of the latter under a non-follower force has been mathematically formulated and analyzed by Wang (2002). The effects of the location and size of the piezoelectric layers on the enhancement are studied.

The enhancement of Beck's column (associated with the flutter phenomenon of a cantilever under a follower force) using piezoelectric layers has not been previously presented. This paper deals with the flutter and buckling enhancement of a column, fixed at one end and constrained elastically at the other end, subjected to a follower force using a pair of piezoelectric layers. The mathematical formulation is first presented and then solved numerically to illustrate the effect of parameters such as applied voltage, length and position of actuators and the spring stiffness. The influence of these parameters on the amount of strength enhancement and the transition between flutter and buckling instability is discussed.

2. Problem description

Fig. 1 shows a column with width b, thickness h, length L, density ρ and isotropic with Young's modulus E that has a pair of piezoelectric patches bonded on its surfaces. Each piezoelectric layer has thickness h_1, density ρ', Young's modulus E_p and equivalent piezoelectric coefficient for one-dimensional problem $\bar{e}_{31}$. Let x denotes the coordinate along the length of the column with its origin at the left end, and $w(x)$ the deflection of the beam, defined to be positive downward. The piezoelectric layers are located from $x = L_1$ to L_2. The column is fixed at $x = 0$ and constrained transversely by a spring with stiffness coefficient k at $x = L$.

For buckling problems, L/h is usually large and the effects of shear deformation and rotary inertia may be neglected. Therefore, the displacement field of the column is written as

$$u_x(x,t) = -z\frac{\partial w(x,t)}{\partial x}, \tag{1}$$

where $w(x,t)$ and $u_x(x,t)$ are the displacements in the transverse z-direction and longitudinal x-direction, respectively. The amplitude of the strain ε_x, stress σ_x, and the moment M_x in the column due to w are given by

$$\varepsilon_x = -z\frac{\partial^2 w}{\partial x^2}, \tag{2}$$

$$\sigma_x = -Ez\frac{\partial^2 w}{\partial x^2}, \tag{3}$$

$$M_x = \int_{-\frac{h}{2}}^{\frac{h}{2}} z\sigma_x \,\mathrm{d}z = -EI\frac{\partial^2 w}{\partial x^2}, \tag{4}$$

where $I = (1/12)bh^3$.

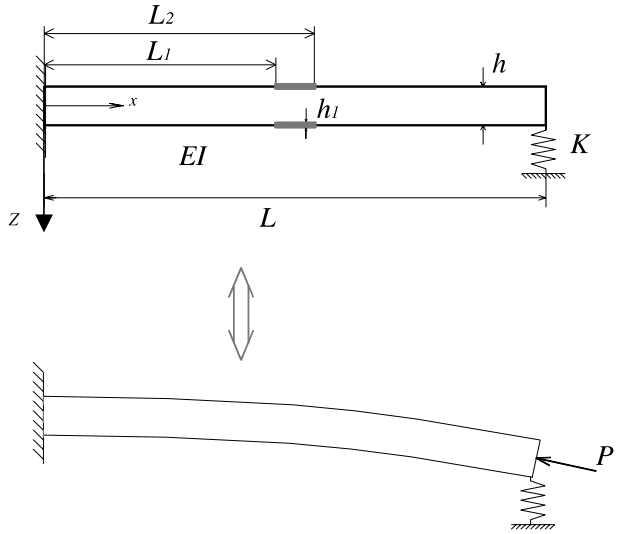

Fig. 1. Column with a pair of piezoelectric layers under follower force.

The stress in the piezoelectric layer accounting for electro-mechanical effects can be expressed as (Crawley and de Luis, 1987)

$$\bar{\sigma}_x = -E_p z \frac{\partial^2 \overline{w}}{\partial x^2} - \bar{e}_{31} E_z, \tag{5}$$

where the over-bar represents the variations in the piezoelectric layer and E_z is the electric field in the piezoelectric layer. The stress given by the first term on the right hand side of Eq. (5) results in a moment $\bar{M}_x$ on the column induced by w and can be approximately expressed as

$$\bar{M}_x = -E_p hbh_1 \left(\frac{h}{2} + h_1 \right) \frac{\partial^2 w}{\partial x^2}. \tag{6}$$

If the piezoelectric layers are placed symmetrically and poled in the transverse direction of the column, then applying equal voltages V to the upper and lower piezoelectric layers will induce tensile mechanical stresses on the column if complete bonding is assumed, as pointed out by Crawley and de Luis (1987). This stress is given by the second term on the right hand side of Eq. (5) and effect in concentrated tensile forces at $x = L_1$ and L_2, each given by

$$F = -2bh_1 E_z \bar{e}_{31} = -2b\bar{e}_{31} V, \tag{7}$$

where $E_z = V/h_1$. Such tensile force induced by the piezoelectric layer may be used to enhance the flutter and buckling of the column subjected to a compressive follower force P at $x = L$.

3. Mathematical model for flutter and buckling analysis of enhanced column

For clarity, the column is considered to comprise three parts with the deflections denoted by $w_1(x)$ for $0 \leqslant x \leqslant L_1$, $w_2(x)$ for $L_1 \leqslant x \leqslant L_2$ and $w_3(x)$ for $L_2 \leqslant x \leqslant L$. The governing equations for the column subjected to a follower force can be expressed as

$$EI \frac{\partial^4 w_1}{\partial x^4} + P \frac{\partial^2 w_1}{\partial x^2} + \rho bh \frac{\partial^2 w_1}{\partial t^2} = 0, \tag{8}$$

$$(EI)' \frac{\partial^4 w_2}{\partial x^4} + (P - F) \frac{\partial^2 w_2}{\partial x^2} + (\rho bh + 2\rho' bh_1) \frac{\partial^2 w_2}{\partial t^2} = 0, \tag{9}$$

$$EI \frac{\partial^4 w_3}{\partial x^4} + P \frac{\partial^2 w_3}{\partial x^2} + \rho bh \frac{\partial^2 w_3}{\partial t^2} = 0, \tag{10}$$

where $(EI)' = EI + E_p hbh_1((h/2) + h_1)$.

The general solution of Eqs. (8)–(10) can be written as

$$w_j(x,t) = W_j(x) e^{i\omega t} \quad j = 1, 2, 3, \tag{11}$$

where $W_j(x)$ is the admissible shape vibrating at the circular frequency ω of the column. Substituting Eq. (11) into Eqs. (8)–(10) yields the governing equation for $W_j(x)$

$$EI \frac{d^4 W_1}{dx^4} + P \frac{d^2 W_1}{dx^2} - \rho bh\omega^2 W_1 = 0, \tag{12}$$

$$(EI)' \frac{d^4 W_2}{dx^4} + (P - F) \frac{d^2 W_2}{dx^2} - \left(\rho bh + 2\rho' bh_1\right)\omega^2 W_2 = 0, \tag{13}$$

$$EI \frac{d^4 W_3}{dx^4} + P \frac{d^2 W_3}{dx^2} - \rho bh\omega^2 W_3 = 0. \tag{14}$$

The solutions for W_1 and W_3 are given by

$$W_1(x) = A_1 \cos k_1 x + A_2 \sin k_1 x + A_3 \cosh k_2 x + A_4 \sinh k_2 x, \tag{15}$$

$$W_3(x) = C_1 \cos k_1 x + C_2 \sin k_1 x + C_3 \cosh k_2 x + C_4 \sinh k_2 x, \tag{16}$$

where $k_1 = \sqrt{\left(\mu^2 + \lambda^4/4\right)^{1/2} + \lambda^2/2}$, $k_2 = \sqrt{\left(\mu^2 + \lambda^4/4\right)^{1/2} - \lambda^2/2}$, $\lambda^2 = P/EI$ and $\mu^2 = \rho bh\omega^2/EI$. The solution for W_2 depends on the relative magnitude between P and F, and is found to be

$$W_2(x) = B_1 \cos \bar{k}_1 x + B_2 \sin \bar{k}_1 x + B_3 \cosh \bar{k}_2 x + B_4 \sinh \bar{k}_2 x \quad \text{when } P \geqslant F, \tag{17}$$

$$W_2(x) = B_1 \cosh \bar{k}_1 x + B_2 \sinh \bar{k}_1 x + B_3 \cos \bar{k}_2 x + B_4 \sin \bar{k}_2 x \quad \text{when } P < F, \tag{18}$$

where $\bar{k}_1 = \sqrt{\left(\bar{\mu}^2 + \bar{\lambda}^4/4\right)^{1/2} + \bar{\lambda}^2/2}$, $\bar{k}_2 = \sqrt{\left(\bar{\mu}^2 + \bar{\lambda}^4/4\right)^{1/2} - \bar{\lambda}^2/2}$, $\bar{\lambda}^2 = P - F/(EI)'$ and $\bar{\mu}^2 = (\rho bh + 2\rho' bh_1)\omega^2/(EI)'$.

The flutter and buckling capacities of the piezoelectric-enhanced column can be obtained using the condition for the non-trivial solution for the deflection (or equivalently A_i, B_i and C_i, $i = 1, 2, 3, 4$) after imposing the boundary conditions.

4. Analytical solution for flutter and buckling capacity of enhanced column

For the column of Fig. 1, there are four boundary and eight continuity conditions. At $x = 0$, the fixed end condition translates to

$$W_1|_{x=0} = 0 \quad \left.\frac{\mathrm{d}W_1}{\mathrm{d}x}\right|_{x=0} = 0, \tag{19}$$

whereas at $x = L$, the vertical spring constraint implies that

$$\left.\frac{\mathrm{d}^2 W_3}{\mathrm{d}x^2}\right|_{x=L} = 0 \quad \left.\frac{\mathrm{d}^3 W_3}{\mathrm{d}x^3}\right|_{x=L} - \frac{\zeta^2}{L^3} W_3|_{x=L} = 0, \tag{20}$$

where $\zeta^2 = kL^3/EI$. The continuity conditions for the three segments can be written as follows. At $x = L_1$,

$$\begin{aligned} &W_1|_{x=L_1} = W_2|_{x=L_1} \quad \left.\frac{\mathrm{d}W_1}{\mathrm{d}x}\right|_{x=L_1} = \left.\frac{\mathrm{d}W_2}{\mathrm{d}x}\right|_{x=L_1} \\ &\left.\frac{\mathrm{d}^2 W_1}{\mathrm{d}x^2}\right|_{x=L_1} = \left.\frac{\mathrm{d}^2 W_2}{\mathrm{d}x^2}\right|_{x=L_1} \quad \left.\frac{\mathrm{d}^3 W_1}{\mathrm{d}x^3}\right|_{x=L_1} = \left.\frac{\mathrm{d}^3 W_2}{\mathrm{d}x^3}\right|_{x=L_1} \end{aligned} \tag{21}$$

and at $x = L_2$,

$$\begin{aligned} &W_2|_{x=L_2} = W_3|_{x=L_2} \quad \left.\frac{\mathrm{d}W_2}{\mathrm{d}x}\right|_{x=L_2} = \left.\frac{\mathrm{d}W_3}{\mathrm{d}x}\right|_{x=L_2} \\ &\left.\frac{\mathrm{d}^2 W_2}{\mathrm{d}x^2}\right|_{x=L_2} = \left.\frac{\mathrm{d}^2 W_3}{\mathrm{d}x^2}\right|_{x=L_2} \quad \left.\frac{\mathrm{d}^3 W_2}{\mathrm{d}x^3}\right|_{x=L_2} = \left.\frac{\mathrm{d}^3 W_3}{\mathrm{d}x^3}\right|_{x=L_2}. \end{aligned} \tag{22}$$

Substituting Eqs. (15)–(18) into the 12 conditions given in Eqs. (19)–(22) leads to a set of twelve homogenous equations, which can be expressed in the following form

$$\begin{bmatrix}
r_{11} & & r_{13} & & & & & & & & & \\
 & r_{22} & & r_{24} & & & & & & & & \\
 & & & & & & & & r_{39} & r_{3,10} & r_{3,11} & r_{3,12} \\
 & & & & & & & & r_{49} & r_{4,10} & r_{4,11} & r_{4,12} \\
r_{51} & r_{52} & r_{53} & r_{54} & r_{55} & r_{56} & r_{57} & r_{58} & & & & \\
r_{61} & r_{62} & r_{63} & r_{64} & r_{65} & r_{66} & r_{67} & r_{68} & & & & \\
r_{71} & r_{72} & r_{73} & r_{74} & r_{75} & r_{76} & r_{77} & r_{78} & & & & \\
r_{81} & r_{82} & r_{83} & r_{84} & r_{85} & r_{86} & r_{87} & r_{88} & & & & \\
 & & & & r_{95} & r_{96} & r_{97} & r_{98} & r_{99} & r_{9,10} & r_{9,11} & r_{9,12} \\
 & & & & r_{10,5} & r_{10,6} & r_{10,7} & r_{10,8} & r_{10,9} & r_{10,10} & r_{10,11} & r_{10,12} \\
 & & & & r_{11,5} & r_{11,6} & r_{11,7} & r_{11,8} & r_{11,9} & r_{11,10} & r_{11,11} & r_{11,12} \\
 & & & & r_{12,5} & r_{12,6} & r_{12,7} & r_{12,8} & r_{12,9} & r_{12,10} & r_{12,11} & r_{12,12}
\end{bmatrix}
\begin{Bmatrix} A_1 \\ A_2 \\ A_3 \\ A_4 \\ B_1 \\ B_2 \\ B_3 \\ B_4 \\ C_1 \\ C_2 \\ C_3 \\ C_4 \end{Bmatrix} = [R] \begin{Bmatrix} A_1 \\ A_2 \\ A_3 \\ A_4 \\ B_1 \\ B_2 \\ B_3 \\ B_4 \\ C_1 \\ C_2 \\ C_3 \\ C_4 \end{Bmatrix}$$

$$= \begin{Bmatrix} 0 \\ 0 \\ 0 \\ 0 \\ 0 \\ 0 \\ 0 \\ 0 \\ 0 \\ 0 \\ 0 \\ 0 \end{Bmatrix} \quad \text{for } P \geqslant F, \tag{23a}$$

$$\begin{bmatrix}
r_{11} & & r_{13} & & & & & & & & & \\
 & r_{22} & & r_{24} & & & & & & & & \\
 & & & & & & & & r_{39} & r_{3,10} & r_{3,11} & r_{3,12} \\
 & & & & & & & & r_{49} & r_{4,10} & r_{4,11} & r_{4,12} \\
r_{51} & r_{52} & r_{53} & r_{54} & \bar{r}_{55} & \bar{r}_{56} & \bar{r}_{57} & \bar{r}_{58} & & & & \\
r_{61} & r_{62} & r_{63} & r_{64} & \bar{r}_{65} & \bar{r}_{66} & \bar{r}_{67} & \bar{r}_{68} & & & & \\
r_{71} & r_{72} & r_{73} & r_{74} & \bar{r}_{75} & \bar{r}_{76} & \bar{r}_{77} & \bar{r}_{78} & & & & \\
r_{81} & r_{82} & r_{83} & r_{84} & \bar{r}_{85} & \bar{r}_{86} & \bar{r}_{87} & \bar{r}_{88} & & & & \\
 & & & & \bar{r}_{95} & \bar{r}_{96} & \bar{r}_{97} & \bar{r}_{98} & r_{99} & r_{9,10} & r_{9,11} & r_{9,12} \\
 & & & & \bar{r}_{10,5} & \bar{r}_{10,6} & \bar{r}_{10,7} & \bar{r}_{10,8} & r_{10,9} & r_{10,10} & r_{10,11} & r_{10,12} \\
 & & & & \bar{r}_{11,5} & \bar{r}_{11,6} & \bar{r}_{11,7} & \bar{r}_{11,8} & r_{11,9} & r_{11,10} & r_{11,11} & r_{11,12} \\
 & & & & \bar{r}_{12,5} & \bar{r}_{12,6} & \bar{r}_{12,7} & \bar{r}_{12,8} & r_{12,9} & r_{12,10} & r_{12,11} & r_{12,12}
\end{bmatrix}
\begin{Bmatrix} A_1 \\ A_2 \\ A_3 \\ A_4 \\ B_1 \\ B_2 \\ B_3 \\ B_4 \\ C_1 \\ C_2 \\ C_3 \\ C_4 \end{Bmatrix}$$

$$= [\bar{R}] \begin{Bmatrix} A_1 \\ A_2 \\ A_3 \\ A_4 \\ B_1 \\ B_2 \\ B_3 \\ B_4 \\ C_1 \\ C_2 \\ C_3 \\ C_4 \end{Bmatrix} = \begin{Bmatrix} 0 \\ 0 \\ 0 \\ 0 \\ 0 \\ 0 \\ 0 \\ 0 \\ 0 \\ 0 \\ 0 \\ 0 \end{Bmatrix} \quad \text{for } P < F, \tag{23b}$$

where r_{ij} ($i = 1, 2, \ldots, 12$; $j = 1, 2, \ldots, 12$) and $\bar{r}_{kl}$ ($k = 5, 6, \ldots, 12$; $l = 5, 6, 7, 8$) are listed in the appendix, and all the unfilled places in the above matrices indicate the value of zero.

For non-trivial solution of the vector $(A_1, \ldots, A_4, B_1, \ldots, B_4, C_1, \ldots, C_4)^{\mathrm{T}}$, the following conditions are imposed

$$\det[R] = 0 \quad \text{for } P \geqslant F, \tag{24a}$$

$$\det[\bar{R}] = 0 \quad \text{for } P < F. \tag{24b}$$

Theoretically, this will give the vibration frequencies of the system. The load at which the fundamental frequency is zero corresponds to the buckling capacity whereas the load at which the first two frequencies are equal gives the flutter capacity. These capacities can be obtained numerically as follows. For a given piezoelectric material and applied voltage V, the tensile force F induced on the column by the piezoelectric layers can be computed using Eq. (7). For prescribed values of L_1, L_2 and follower force P, the first two resonant frequencies ω_1 and ω_2 are numerically estimated using Eq. (24a) or Eq. (24b). By varying P, set of values for ω_1 and ω_2 are computed and plotted, from which the flutter and buckling capacity of the column can be deduced. The effectiveness of the piezoelectric layer in enhancing the flutter and buckling capacity in the column can be demonstrated by changing V, L_1 and L_2.

5. Numerical simulation and discussions

As an illustration, a steel column with PZT-4 piezoelectric actuator attached is considered with the geometric and material constants listed in Table 1. The results are presented in non-dimensional form where the non-dimensional frequency of the column, the compressive follower force, the tensile force induced by the piezoelectric layer and the spring constant are defined as follows: $\bar{\omega} = \rho bh\omega^2 L^4/EI$, $\bar{P} = P/P_{\mathrm{cr}}$, $\bar{F} = F/P_{\mathrm{cr}}$, and $\zeta^2 = kL^3/EI$, where $P_{\mathrm{cr}} = \pi^2 EI/L^2$ is the Euler buckling load of the original column. Note that $\zeta^2 = 0$ corresponds to a free standing column whereas $\zeta^2 \to \infty$ is for a column propped at one end.

First, consider the case of a column with $\bar{F} = 0$ and $h_1 = 0$, implying that no piezoelectric layer is attached. The two extreme cases of $\zeta^2 = 0$ and $\zeta^2 \to \infty$ under the action of P can be solved, giving the column capacity of $\bar{P} = 2.035$ and 2.040 respectively. These values compare well with the values of $\bar{P} = 2.034$ and 2.045 respectively provided by Timoshenko and Gere (1961). For other values of ζ^2, the variations of the first two frequencies of the column ω_1 and ω_2 with P are plotted in Fig. 2. For $\zeta^2 < 36$, it is found that ω_1 and ω_2

Table 1
Geometrical and material properties of column and the piezoelectric layer

	Column	Piezoelectric layer
Length (m)	1.0	–
Width (m)	0.08	0.08
Height (m)	0.002	0.0001
Young's modulus (N/m^2)	78.0×10^9	–
Poisson's ratio	0.29	0.30
Mass density (kg/m^3)	7800	7500
e_{31} (C/m^2)	–	−4.1
e_{33} (C/m^2)	–	14.1
$\bar{e}_{31}$ (C/m^2)	–	−9.29
c_{11} (N/m^2)	–	13.2×10^9
c_{33} (N/m^2)	–	11.5×10^9
c_{12} (N/m^2)	–	7.1×10^9
c_{13} (N/m^2)	–	7.3×10^9
E_{p} (N/m^2)	–	78.6

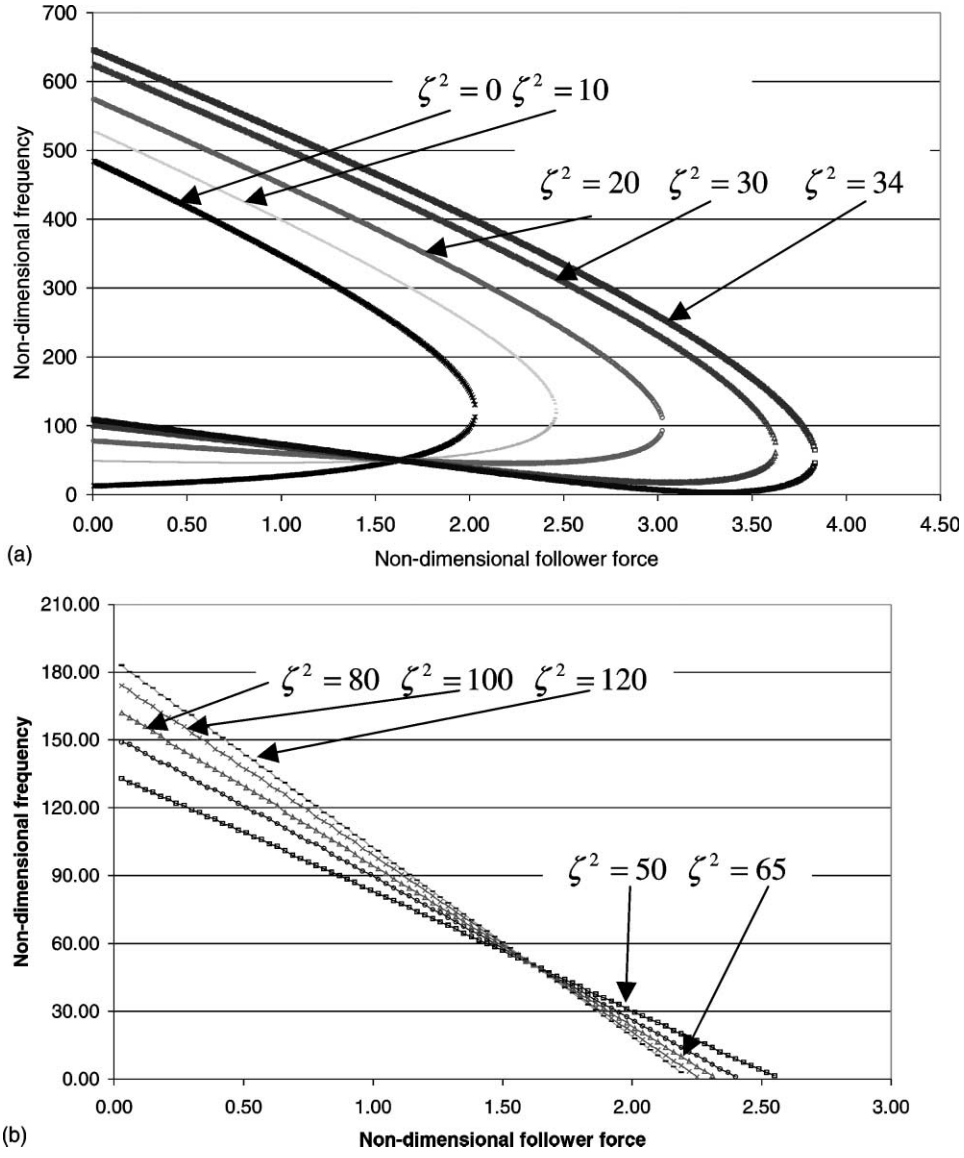

Fig. 2. (a) First two resonant frequencies versus follower force. (b) First resonant frequency versus follower force.

approach each other without passing through zero, as shown in Fig. 2(a) indicating that the column flutters but does not buckle. For higher values of ζ^2, the beam buckles first (i.e. frequency approaches zero first), as shown in Fig. 2(b). This trend is reasonable because when the free end is under some restraint, there is lesser tendency to flutter. The values of P at which ω_1 first reaches zero or equals to ω_2 as P is increased for different ζ^2 are plotted in Fig. 3, indicating that a transition value of $\zeta^2 \approx 36$, below which the beam flutters and above which the beam buckles. It can be seen that the drop in the capacity of the column just after the transit point is steep, from flutter to buckling. These results agree with those in Kounadis (1983).

For the case where the piezoelectric layers are attached with $L_1 = 0.1$ m and $L_2 = 0.9$ m, the capacity of the column with external voltage applied under different degree of restraint are plotted in Fig. 4. Fig. 4(a)

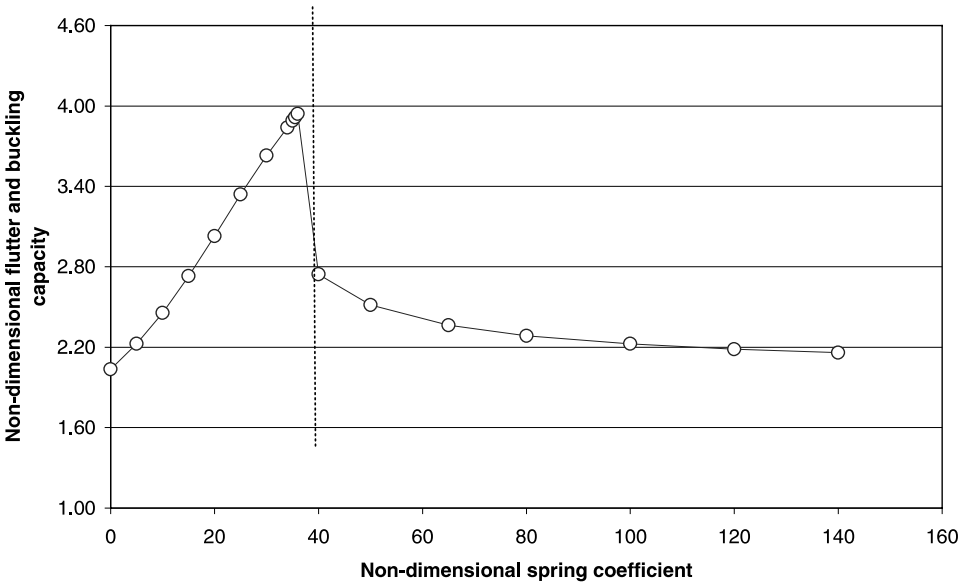

Fig. 3. Flutter and buckling capacity of column versus spring stiffness.

shows the increase in both flutter and buckling strength of the column as the applied voltage is increased from 0 to 50V. Fig. 4(b) indicates that the percentage increase with respect to a column without piezoelectric layers ranges from about 12% to 45%. Without external voltages, the piezoelectric layers increase the stiffness of the column locally and contribute about 12% to the strength increase. Hence, the electromechanical effect of the piezoelectric layer can be substantial when external voltages are applied to the layer.

As an indication of the size effect, the capacity of the column for three lengths of the piezoelectric layers, namely $L_2 = 0.3$ m, $L_2 = 0.7$ m, and $L_2 = 0.9$ m, are plotted in Fig. 5, for L_1 fixed at 0.1 m. As expected, the capacity increases with size but the flutter capacity does not vary much from $L_2 = 0.7$ to 0.9 m. This is because increasing the stiffness of the column through the piezoelectric layers near the free end is less effective than increasing at the fixed end against flutter while the opposite can be said with respect to buckling.

This is further illustrated by fixing the actuator length (0.4 m) and changing the position, where the values for $L_1 = 0.2$ m and $L_1 = 0.5$ m are plotted in Fig. 6(a) for external voltage of 30 V. The case without actuator is also plotted for comparison purpose. It can be seen that placing the actuator towards the right increases the buckling capacity significantly (by 51%). Placing the actuator towards the left increases the flutter load by 23%.

The effect of position on the transition value of ζ^2 is also illustrated, where the value decreases when the actuator is placed more towards the fixed end. Hence, for $\zeta^2 = 36$ (corresponding to the transition value of the column without actuator), depending on where the piezoelectric layers are attached, the column can either buckle or fail by flutter. This is also illustrated in Fig. 6(b) in which the variations of the first two frequencies are calculated for $\zeta^2 = 36$.

As a further illustration of the above effects, the results for the cases of $L_1 = 0.5$ m and $L_2 = 0.9$ m, and $L_1 = 0.1$ m and $L_2 = 0.9$ m are plotted in Fig. 7(a). The longer layer does not produce significant increase in the buckling capacity but significantly increase the flutter load by virtual of its position. In addition, the relative position of the transition point is consistent with the earlier discussion. The transition between the form of instability for $\zeta^2 = 39$ is illustrated by the variation of the first two frequencies plotted in Fig. 7(b).

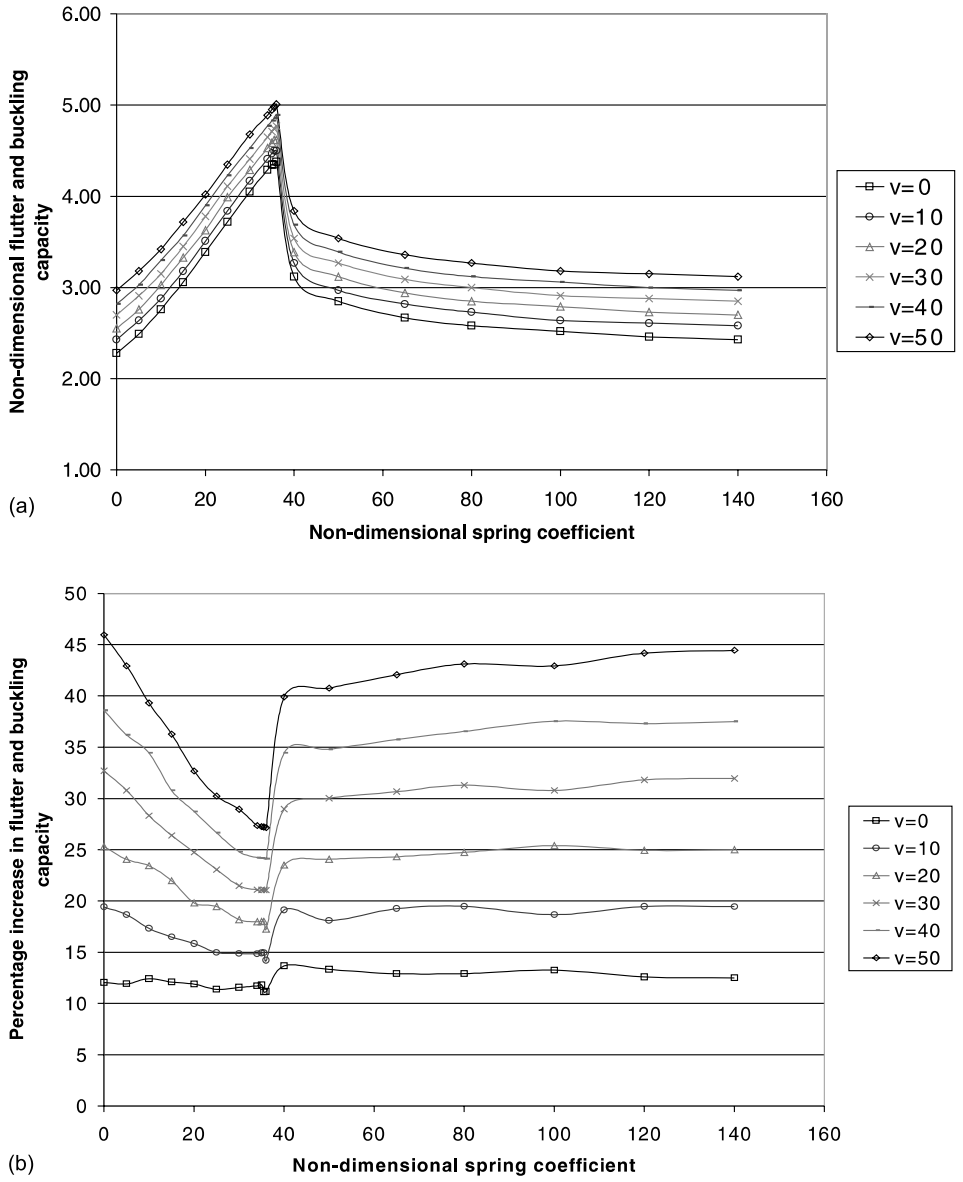

Fig. 4. (a) Flutter and buckling capacity of column at different voltages when $L_1 = 0.1$ and $L_2 = 0.9$. (b) The percentage increase in flutter and buckling capacity of column.

6. Concluding remarks

By presenting the mathematical formulation and numerical solution of the flutter and buckling analysis, the effectiveness of a pair of surface-bonded piezoelectric patches to enhance the capacity of a column subjected to a follower force is illustrated. The solution is first validated for the case of a virgin column. It is shown that the degree of transverse restraint at the free end determines the form of instability. The presence

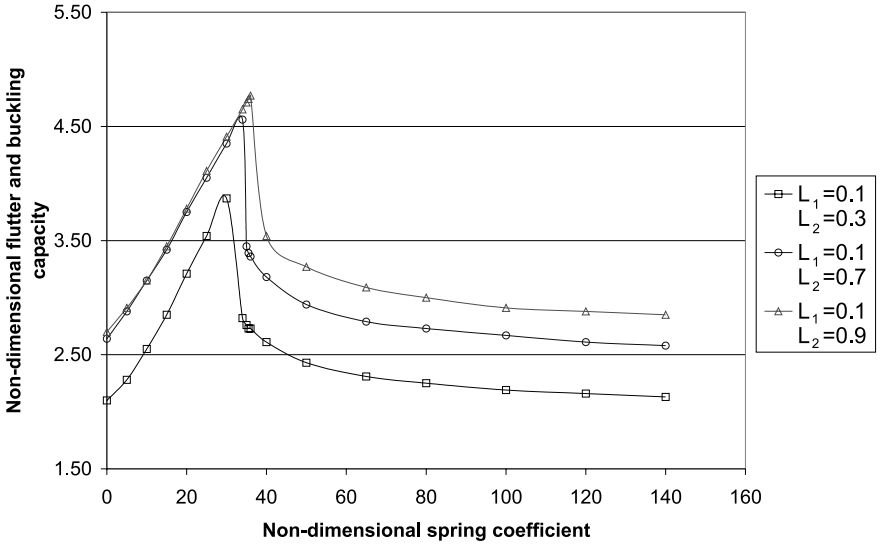

Fig. 5. Flutter and buckling capacity of column for different sizes of piezoelectric layer at $V = 30$.

of the piezoelectric layers not only increases the strength of the column but can also alter the form of instability. Whilst longer layers lead to higher capacity in general, placing the actuators towards the fixed end is more effective in increasing the flutter capacity whilst placing them away from the fixed end results in a substantial increase in the buckling capacity. Hence, in view of the steep drop in capacity at the transition stiffness, the results of this study show the importance of proper placement of piezoelectric patches to ensure optimal strength enhancement.

Acknowledgements

The authors are grateful to the reviewers for their constructive comments.

Appendix A. Elements of the matrix

$$r_{11} = 1, \quad r_{13} = 1, \quad r_{22} = k_1, \quad r_{24} = k_2,$$

$$r_{39} = -k_1^2 \cos k_1 L, \quad r_{3,10} = -k_1^2 \sin k_1 L, \quad r_{3,11} = k_2^2 \cosh k_2 L, \quad r_{3,12} = k_2^2 \sinh k_2 L,$$

$$r_{4,9} = k_1^3 \sin k_1 L - \frac{\zeta^2}{L^3} \cos k_1 L, \quad r_{4,10} = -k_1^3 \cos k_1 L - \frac{\zeta^2}{L^3} \sin k_1 L,$$

$$r_{4,11} = k_2^3 \sinh k_2 L - \frac{\zeta^2}{L^3} \cosh k_2 L, \quad r_{4,12} = k_2^3 \cosh k_2 L - \frac{\zeta^2}{L^3} \sinh k_2 L,$$

$$r_{51} = \cos k_1 L_1, \quad r_{52} = \sin k_1 L_1, \quad r_{53} = \cosh k_2 L_1, \quad r_{54} = \sinh k_2 L_1,$$

$$r_{55} = -\cos \bar{k}_1 L_1, \quad r_{56} = -\sin \bar{k}_1 L_1, \quad r_{57} = -\cosh \bar{k}_2 L_1, \quad r_{58} = -\sinh \bar{k}_2 L_1,$$

$$r_{61} = -k_1 \sin k_1 L_1, \quad r_{62} = k_1 \cos k_1 L_1, \quad r_{63} = k_2 \sinh k_2 L_1, \quad r_{64} = k_2 \cosh k_2 L_1, \quad r_{65} = \bar{k}_1 \sin \bar{k}_1 L_1,$$

$$r_{66} = -\bar{k}_1 \cos \bar{k}_1 L_1, \quad r_{67} = -\bar{k}_2 \sinh \bar{k}_2 L_1, \quad r_{68} = -\bar{k}_2 \cosh \bar{k}_2 L_1,$$

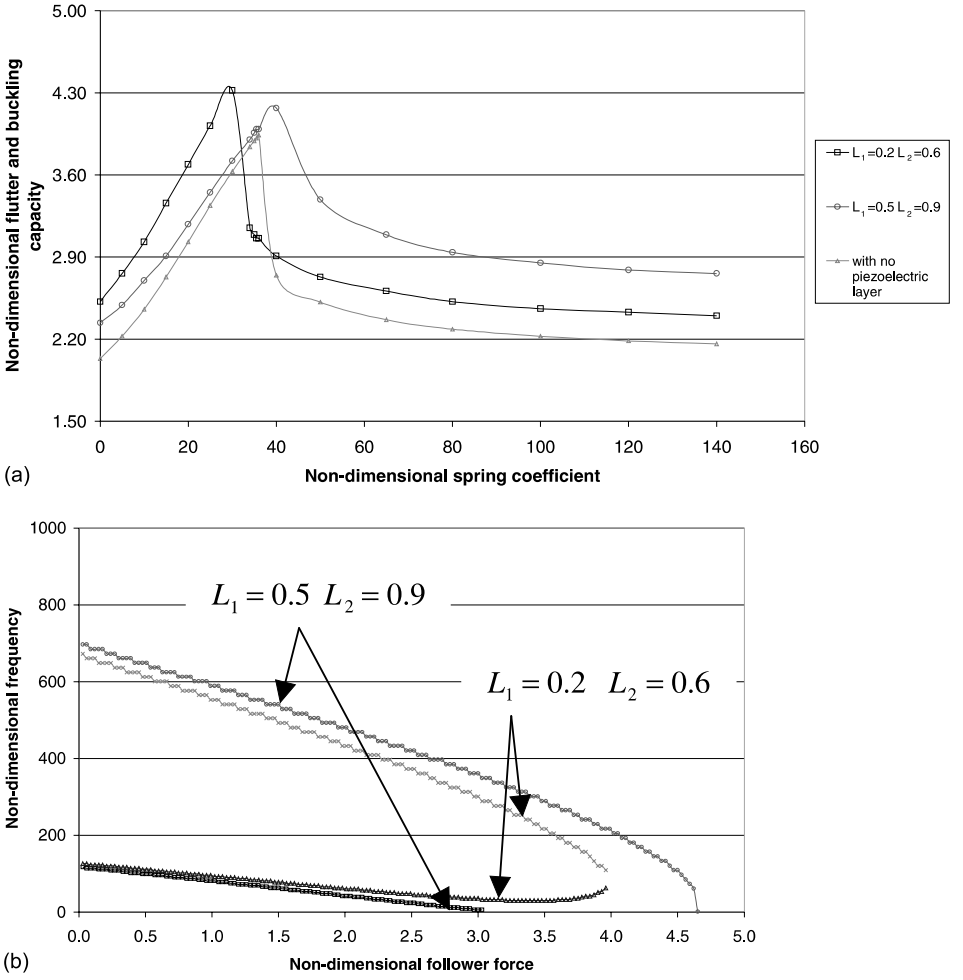

Fig. 6. (a) Flutter and buckling capacity of column at different location of the piezoelectric layer at $V = 30$. (b) First and second frequencies of column for different locations of piezoelectric layer at $V = 30$.

$$
\begin{aligned}
&r_{71} = -k_1^2 \cos k_1 L_1, \quad r_{72} = -k_1^2 \sin k_1 L_1, \quad r_{73} = k_2^2 \cosh k_2 L_1, \quad r_{74} = k_2^2 \sinh k_2 L_1,\\
&r_{75} = \bar{k}_1^2 \cos \bar{k}_1 L_1, \quad r_{76} = \bar{k}_1^2 \sin \bar{k}_1 L_1, \quad r_{77} = -\bar{k}_2^2 \cosh \bar{k}_2 L_1, \quad r_{78} = -\bar{k}_2^2 \sinh \bar{k}_2 L_1,\\
&r_{81} = k_1^3 \sin k_1 L_1, \quad r_{82} = -k_1^3 \cos k_1 L_1, \quad r_{83} = k_2^3 \sinh k_2 L_1, \quad r_{84} = k_2^3 \cosh k_2 L_1,\\
&r_{85} = -\bar{k}_1^3 \sin \bar{k}_1 L_1, \quad r_{86} = \bar{k}_1^3 \cos \bar{k}_1 L_1, \quad r_{87} = -\bar{k}_2^3 \sinh \bar{k}_2 L_1, \quad r_{88} = -\bar{k}_2^3 \cosh \bar{k}_2 L_1,\\
&r_{95} = -\cos \bar{k}_1 L_2, \quad r_{96} = -\sin \bar{k}_1 L_2, \quad r_{97} = -\cosh \bar{k}_2 L_2, \quad r_{98} = -\sinh \bar{k}_2 L_2,\\
&r_{99} = \cos k_1 L_2, \quad r_{9,10} = \sin k_1 L_2, \quad r_{9,11} = \cosh k_2 L_2, \quad r_{9,12} = \sinh k_2 L_2,\\
&r_{10,5} = \bar{k}_1 \sin \bar{k}_1 L_2, \quad r_{10,6} = -\bar{k}_1 \cos \bar{k}_1 L_2, \quad r_{10,7} = -\bar{k}_2 \sinh \bar{k}_2 L_2, \quad r_{10,8} = -\bar{k}_2 \cosh \bar{k}_2 L_2,\\
&r_{10,9} = -k_1 \sin k_1 L_2, \quad r_{10,10} = k_1 \cos k_1 L_2, \quad r_{10,11} = k_2 \sinh k_2 L_2, \quad r_{10,12} = k_2 \cosh k_2 L_2,\\
&r_{11,5} = \bar{k}_1^2 \cos \bar{k}_1 L_2, \quad r_{11,6} = \bar{k}_1^2 \sin \bar{k}_1 L_2, \quad r_{11,7} = -\bar{k}_2^2 \cosh \bar{k}_2 L_2, \quad r_{11,8} = -\bar{k}_2^2 \sinh \bar{k}_2 L_2,\\
&r_{11,9} = -k_1^2 \cos k_1 L_2, \quad r_{11,10} = -k_1^2 \sin k_1 L_2, \quad r_{11,11} = k_2^2 \cosh k_2 L_2, \quad r_{11,12} = k_2^2 \sinh k_2 L_2,
\end{aligned}
$$

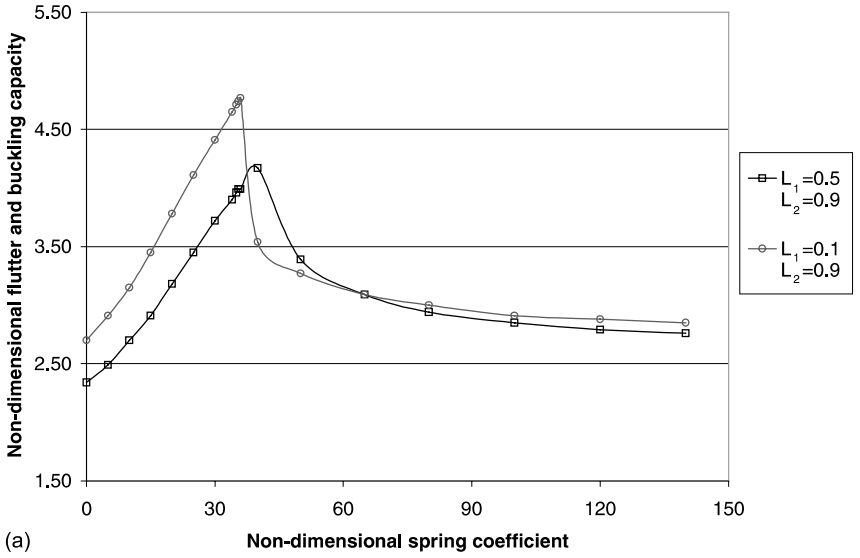

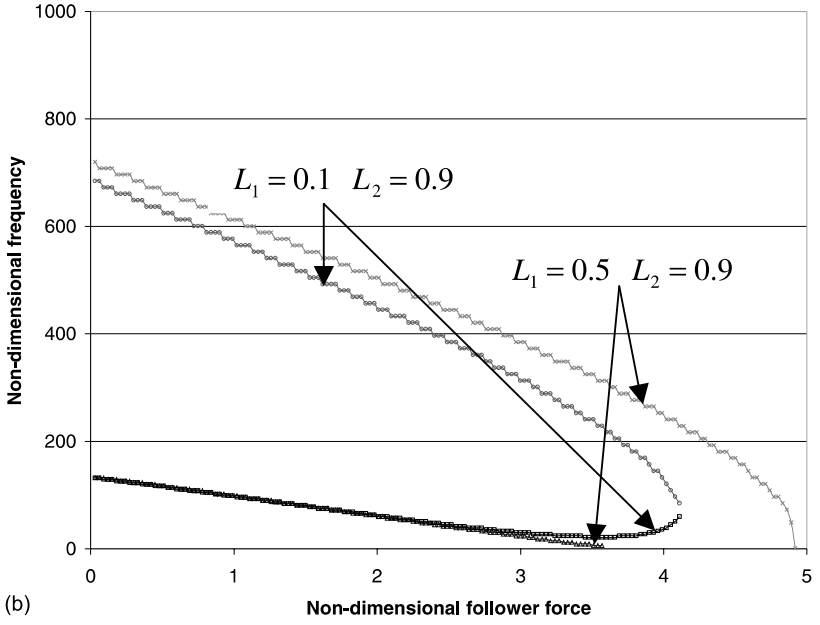

Fig. 7. (a) Flutter and buckling capacity of column at $V = 30$. (b) First and second frequencies of column at $V = 30$.

$$r_{12,5} = -\bar{k}_1^3 \sin \bar{k}_1 L_2, \quad r_{12,6} = \bar{k}_1^3 \cos \bar{k}_1 L_2, \quad r_{12,7} = -\bar{k}_2^3 \sinh \bar{k}_2 L_2, \quad r_{12,8} = -\bar{k}_2^3 \cosh \bar{k}_2 L_2,$$
$$r_{12,9} = k_1^3 \sin k_1 L_2, \quad r_{12,10} = -k_1^3 \cos k_1 L_2, \quad r_{12,11} = k_2^3 \sinh k_2 L_2, \quad r_{12,12} = k_2^3 \cosh k_2 L_2,$$
$$\bar{r}_{55} = -\cosh \bar{k}_1 L_1, \quad \bar{r}_{56} = -\sinh \bar{k}_1 L_1, \quad \bar{r}_{57} = -\cos \bar{k}_2 L_1, \quad \bar{r}_{58} = -\sin \bar{k}_2 L_1,$$
$$\bar{r}_{65} = -\bar{k}_1 \sinh \bar{k}_1 L_1, \quad \bar{r}_{66} = -\bar{k}_1 \cosh \bar{k}_1 L_1, \quad \bar{r}_{67} = \bar{k}_2 \sin \bar{k}_2 L_1, \quad \bar{r}_{68} = -\bar{k}_2 \cos \bar{k}_2 L_1,$$
$$\bar{r}_{75} = -\bar{k}_1^2 \cosh \bar{k}_1 L_1, \quad \bar{r}_{76} = -\bar{k}_1^2 \sinh \bar{k}_1 L_1, \quad \bar{r}_{77} = \bar{k}_2^2 \cos \bar{k}_2 L_1, \quad \bar{r}_{78} = \bar{k}_2^2 \sin \bar{k}_2 L_1,$$

$$\bar{r}_{85} = -\bar{k}_1^3 \sinh \bar{k}_1 L_1, \quad \bar{r}_{86} = -\bar{k}_1^3 \cosh \bar{k}_1 L_1, \quad \bar{r}_{87} = -\bar{k}_2^3 \sin \bar{k}_2 L_1, \quad \bar{r}_{88} = \bar{k}_2^3 \cos \bar{k}_2 L_1,$$
$$\bar{r}_{95} = -\cosh \bar{k}_1 L_2, \quad \bar{r}_{96} = -\sinh \bar{k}_1 L_2, \quad \bar{r}_{97} = -\cos \bar{k}_2 L_2, \quad \bar{r}_{98} = -\sin \bar{k}_2 L_2,$$
$$\bar{r}_{10,5} = -\bar{k}_1 \sinh \bar{k}_1 L_2, \quad \bar{r}_{10,6} = -\bar{k}_1 \cosh \bar{k}_1 L_2, \quad \bar{r}_{10,7} = \bar{k}_2 \sin \bar{k}_2 L_2, \quad \bar{r}_{10,8} = -\bar{k}_2 \cos \bar{k}_2 L_2,$$
$$\bar{r}_{11,5} = -\bar{k}_1^2 \cosh \bar{k}_1 L_2, \quad \bar{r}_{11,6} = -\bar{k}_1^2 \sinh \bar{k}_1 L_2, \quad \bar{r}_{11,7} = \bar{k}_2^2 \cos \bar{k}_2 L_2, \quad \bar{r}_{11,8} = \bar{k}_2^2 \sin \bar{k}_2 L_2,$$
$$\bar{r}_{12,5} = -\bar{k}_1^3 \sinh \bar{k}_1 L_2, \quad \bar{r}_{12,6} = \bar{k}_1^3 \cosh \bar{k}_1 L_2, \quad \bar{r}_{12,7} = -\bar{k}_2^3 \sin \bar{k}_2 L_2, \quad \bar{r}_{12,8} = \bar{k}_2^3 \cos \bar{k}_2 L_2.$$

References

Atanackvic, T.M., Cveticanin, L., 1994. Dynamics of in-plane motion of a robot arm. In: Acar, Makra, M.J., Penny, E. (Eds.), Mechatronics. Computational Mechanics Publication, Boston, pp. 147–152.

Beck, M., 1952. Die Knicklast des einseitig eingespannten tangential gedruckten stabes. Z. Angew. Math. Phys. 3.

Bolotin, V.V., 1963. Non-conservative problems of the theory of elastic stability. Macmillan, New York.

Chandrashekhara, K., Bhatia, K., 1993. Active buckling control of smart composite plates—finite-element analysis. Smart Mater. Struct. 2, 31–39.

Chase, J.G., Bhashyam, S., 1999. Optimal stabilization of plate buckling. Smart Mater. Struct. 8, 204–211.

Crawley, E.F., de Luis, J., 1987. Use of piezoelectric actuators as elements of intelligent structures. AIAA J. 25, 1373–1385.

Feodos'ev, V.I., 1953. Selected problems and questions in strength of materials. Gostekhizdat.

Hauger, W., Vetter, K., 1976. Influence of an elastic foundation on the stability of a tangentially loaded column. J. Sound Vibrat. 47, 296–299.

Hanaoka, M., Washizu, K., 1979. Optimum design of Beck's column. Comput. Struct. 11, 473–480.

Kounadis, A.N., 1983. The existence of regions of divergence instability for nonconservative systems under follower forces. Int. J. Solids Struct. 19, 725–733.

Loughlan, J., 1996. The buckling of composite stiffened box sections subjected to compression and bending. Compos. Struct. 35, 101–116.

Matsuda, H., Sakiyama, T., Morita, C., 1993. Variable cross sectional Beck's column subjected to non-conservative load. Zeitschrift fur angwandte Mathematik und Mechanik (ZAMM) 73, 383–385.

Meressi, T., Paden, B., 1993. Buckling control of a flexible beam using piezoelectric actuators. J. Guid. Contr. Dynam. 16, 977–980.

Milsom, R.F., Reilly, N.H.C., Redwood, M., 1977. Analysis of generation and detection of surface and bulk acoustic waves by interdigital transducer. IEEE Trans. Sonics Ultra. SU-24, 147–166.

Monkhouse, R.S.C., Wilcox, P.W., Dalton, R.P., Cawley, P., 2000. The rapid monitoring of structures using interdigital lamb wave transducers. Smart Mater.

Morgan, D.P., 1998. History of SAW devices. IEEE Int. Freq. Contr. Symp. 439–460.

Pfluger, A., 1950. Stabilitats probleme der elastostatik. Springer-Verlag, Berlin, Structures 9, 304–309.

Timoshenko, S.P., Gere, J.M., 1961. Theory of Elastic Stability. McGraw-Hill International Book Company, Singapore.

Thompson, S.P., Loughlan, J., 1995. The active buckling control of some composite column structure strips using piezoceramic actuators. Comput. Struct. 32, 59–67.

Wang, Q., 2002. On buckling of column structures with a pair of piezoelectric layers. Engng. Struct. 24, 199–205.